

Resolution improvement by minimum variance signal enhancement.

Sabine Van Huffel¹, C. Decanniere², H. Chen¹, P. Van Hecke²

¹*ESAT Laboratory, Department of Electrical Engineering, Katholieke Universiteit Leuven, 3001 Heverlee, Belgium.*

²*Biomedical NMR unit, Faculty of Medicine, Katholieke Universiteit Leuven, 3000 Leuven, Belgium.*

1 Introduction

Evaluation and improvement of a signal enhancement algorithm, originally proposed by Tufts, Kumaresan and KIRSTEINS (1982) and recently generalized by CADZOW (1988), are presented. Little prior information is required and the proposed method can be applied as a *preprocessing* step to a large class of subspace-based signal estimation methods.

In essence, the newly proposed algorithm first arranges the data in a very rectangular (instead of a square) Hankel structured matrix in order to make the corresponding signal-only data matrix orthogonal to the noise, then computes a minimum variance (instead of a least squares) estimate of the signal-only data matrix and finally restores the Hankel structure.

Simulations are given demonstrating a significant improvement in resolution performance over Cadzow's method at a comparable parameter accuracy. Moreover, arranging the data in a very rectangular matrix reduces drastically the required computation time. In addition, the newly proposed signal enhancement algorithm is successfully applied to the quantitative time-domain analysis of Nuclear Magnetic Resonance (NMR) data.

2 Algorithms

Consider a vector $X = [x_0, \dots, x_{N-1}]^T$ of N observations given by:

$$X = \check{X} + X_w \quad (2.1)$$

where \check{X} contains the exact signal component and X_w represents the noise. We are interested in estimating \check{X} from the observed data vector X . Let us assume that the exact signal satisfies a model of order K . For example, in exponential data modeling this assumption implies that the N data points

\check{x}_n of \check{X} satisfy the following model function:

$$\check{x}_n = \sum_{k=1}^K c_k z_k^{t_n} = \sum_{k=1}^K (a_k e^{j\phi_k}) e^{(-d_k + j2\pi f_k)t_n} \quad n = 0, \dots, N-1 \quad (2.2)$$

where $j = \sqrt{-1}$ and t_n is the time lapse between the effective time origin and sample x_n . The objective is to estimate the frequencies f_k , damping factors d_k , amplitudes a_k and phases ϕ_k , $k = 1, \dots, K$. Prior to parameter estimation, the data are preprocessed as follows:

Data preprocessing. Arrange the x_n in a Hankel matrix $H_{L \times M}$ with $L \geq M > K$ and $N = L + M - 1$ and compute the Singular Value Decomposition (SVD) (Golub and Van Loan 1989) (V^H is the conjugated transpose of V):

$$H = \begin{bmatrix} x_0 & x_1 & \dots & x_{M-1} \\ x_1 & x_2 & \dots & x_M \\ \vdots & \vdots & \vdots & \vdots \\ x_{L-1} & x_L & \dots & x_{N-1} \end{bmatrix} = U_{L \times L} \Sigma_{L \times M} V_{M \times M}^H \quad (2.3)$$

where $\Sigma = \text{diag}(\sigma_1, \dots, \sigma_M)$, $\sigma_1 \geq \dots \geq \sigma_M$.

Correct the singular values by applying a correction function f_{corr} (see below) and truncate to rank K :

$$H_K = U_1 f_{\text{corr}}(\Sigma_1) V_1^H \quad (2.4)$$

U_1, V_1 are the first K columns of U, V and $\Sigma_1 = \text{diag}(\sigma_1, \dots, \sigma_K)$.

Finally, restoring the Hankel structure of H_K by arithmetic averaging along its antidiagonals yields along its first column and last row the cleaned-up data samples \hat{x}_n . These steps can be repeated iteratively.

Parameter estimation. Estimate now the signal parameters from the cleaned-up \hat{x}_n , e.g. the f_k, d_k, a_k and ϕ_k in (2.2) can be estimated through linear prediction methods (Kumaresan and Tufts 1982; Cadzow and Wilkes 1991; De Beer and Van Ormondt 1992; Van Huffel et al. 1992). A better alternative is Kung's method (Kung et al. 1983), known as HSVD in NMR (De Beer and Van Ormondt 1992), which circumvents polynomial rooting and root selection by representing the signal in a *state space model* setting. An improved variant, based on Total Least Squares (TLS) and called HTLS, is presented in (Van Huffel et al. 1992) and used here. Hereto, the \hat{x}_n are arranged in a Hankel matrix $\hat{H}_{\hat{L} \times \hat{M}}$ where $\hat{L} = \hat{M} + 1$ is chosen to obtain the best parameter accuracy.

Correction function. Choosing $f_{\text{corr}}(\Sigma) = \Sigma$ and $L = \hat{L}$, $M = \hat{M}$ results in *Cadzow's method*, i.e. the singular values are not corrected and the

Hankel matrix used in the preprocessing procedure has the *same* dimensions as the one used in the chosen parameter estimation method.

We call the method *minimum variance (MV) estimation* when

$$L \gg M > K \quad \text{and} \quad f_{\text{corr}}(\Sigma) = (\Sigma^2 - L\sigma_\nu^2 I)\Sigma^{-1} \quad \text{with} \quad \sigma_K^2 > L\sigma_\nu^2$$

This method computes the MV estimate of the signal-only data matrix \check{H} given $H = \check{H} + W$ provided $W^H W$ equals the identity matrix, up to an unknown scalar, and the signal-only data are “orthogonal” to the noise in the sense that $\check{H}^H W = 0$ (De Moor 1993). Although these conditions are never satisfied exactly, they are more and more satisfied with increasing overdetermination provided the noise is white and has bounded fourth moments. That’s the reason why $L \gg M$ is required. σ_ν^2 is the estimated noise variance and can be known exactly or computed either from the last data points provided they are pure noise or from the noise singular values as: $\sigma_\nu^2 = \frac{1}{(M-K)L} \sum_{i=K+1}^M \sigma_i^2$.

Other correction functions, as well as a detailed analysis of the signal enhancement properties of these methods, are presented in (Van Huffel 1992).

Efficiency and extensions. Based on the number of operations involved (Golub and Van Loan 1989), it is easy to see that the *computationally most intensive* part (2.3-2.4) of the algorithm requires significantly less work whenever $L \gg M$. Denote by L_c (M_c) the number of rows (columns) as used in Cadzow’s method, and by L_{mv} (M_{mv}) the number of rows (columns) as used in the MV estimation method. Then the MV estimation method requires roughly only

$$\frac{3L_{\text{mv}}M_{\text{mv}}^2 + 10M_{\text{mv}}^3 + M_{\text{mv}}KL_{\text{mv}}}{7L_cM_c^2 + 4M_c^3 + M_cKL_c} * 100\% \quad (2.5)$$

of the number of flops performed by Cadzow’s method in the preprocessing procedure. Only the highest order terms are considered, hence (2.5) holds for large L , M . E.g. if $N = 128$ and $K = 5$, as in Example 1, then (2.5) implies that preprocessing a 119×10 data matrix H by the MV estimation method is only 2% of the work needed for processing a 65×64 matrix by Cadzow’s method. With Matlab, ratios of 4% were obtained.

The newly presented signal enhancement algorithm can also be applied (after some straightforward changes) to other problems in signal processing, such as sinusoidal modeling and transfer function modeling where the data are ordered in slightly differently structured matrices, and is not restricted to signals embedded in white noise (see (Van Huffel 1992) how to modify the data in order to obtain similar results).

Size of the Hankel matrix. Given N data points x_n to be put in an $L \times M$ Hankel matrix H , what’s the best choice for (L, M) ? The geometrical-statistical analysis presented in (De Moor 1993) suggests choosing L as

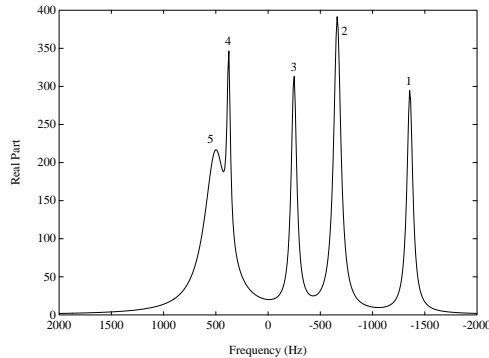


Figure 1. Spectrum of the noise-free simulation signal (real part).

large as possible. However, as M decreases (i.e. L increases) the singular values of the signal-only data matrix \check{H} also decrease, the smallest one quite strongly if $M \approx K$, since \check{H} contains less elements. This implies that the signal-to-noise ratio $\check{\sigma}_K/\sigma_{K+1}$ decreases because the *gap* between the smallest signal singular value $\check{\sigma}_K$ of \check{H} and the largest noise singular value σ_{K+1} of H in (2.3) *narrows enlarging the bias* of the signal subspace estimate of \check{H} . This may have a deteriorating effect on the accuracy of the estimated signal. This implies that M can not be too small. On the other hand, M may not be large since then the signal-only data can not be “orthogonal” to the noise implying that the correction function used in MV estimation is no longer valid. For that reason, we often choose $M \approx 2K$.

3 Simulation results

Example 1. 128 data points, uniformly sampled at 10 kHz, are exactly modeled by a fifth order model function (2.2), given in Table 1 and Fig. 1, and representing a typical *in vivo* ^{31}P NMR signal. The data are perturbed by white Gaussian noise whose real and imaginary components have standard deviation σ_ν . Root Mean-Squared Error (RMSE), bias and standard deviation values of the parameter estimates are computed using 200 noise realizations (excluding failures). A *failure* occurs if *not all peaks are resolved* within the frequency intervals -1379 ± 82 , -685 ± 82 , -271 ± 82 , 353 ± 43 , 478 ± 82 Hz. If respectively no signal enhancement, Cadzow’s method or MV estimation is used prior to HTLS, the method is called P0-HTLS, CA-HTLS or MV-HTLS. During preprocessing, MV-HTLS arranges the data in a 119×10 matrix H while CA-HTLS uses a 65×64 matrix.

Simulations show that MV-HTLS significantly improves the resolution of

Table 1. Bias \pm standard deviation and exact values of the parameter estimates of Example 1. $\sigma_\nu = 1.8$, a.u. stands for arbitrary units and $\psi_k = \phi_k * 180/\pi$ expresses the phase in degrees.

Method	$f_1 = -1379\text{Hz}$	$d_1 = 208\text{Hz}$	$a_1 = 6.1\text{a.u.}$	$\psi_1 = 15^\circ$
CA-HTLS	-0.079 ± 5.166	1.616 ± 33.32	0.070 ± 0.639	0.128 ± 5.884
MV-HTLS	1.371 ± 4.961	0.187 ± 31.35	-0.512 ± 0.564	-1.395 ± 5.645
P0-HTLS	-0.425 ± 5.095	1.099 ± 32.00	0.025 ± 0.591	0.398 ± 5.758
Method	$f_2 = -685\text{Hz}$	$d_2 = 256\text{Hz}$	$a_2 = 9.9\text{a.u.}$	$\psi_2 = 15^\circ$
CA-HTLS	0.272 ± 4.057	-0.104 ± 24.26	0.040 ± 0.671	-0.344 ± 4.019
MV-HTLS	0.506 ± 4.046	-0.104 ± 24.25	-0.383 ± 0.652	-0.411 ± 3.975
P0-HTLS	0.202 ± 4.118	0.330 ± 24.40	0.041 ± 0.668	-0.063 ± 4.007
Method	$f_3 = -271\text{Hz}$	$d_3 = 197\text{Hz}$	$a_3 = 6.0\text{a.u.}$	$\psi_3 = 15^\circ$
CA-HTLS	-0.236 ± 4.810	0.755 ± 27.96	0.113 ± 0.583	-0.116 ± 6.524
MV-HTLS	-0.564 ± 4.723	2.382 ± 27.42	-0.262 ± 0.555	-0.051 ± 6.345
P0-HTLS	-0.486 ± 4.876	0.724 ± 27.51	0.091 ± 0.584	0.390 ± 6.605
Method	$f_4 = 353\text{Hz}$	$d_4 = 117\text{Hz}$	$a_4 = 2.8\text{a.u.}$	$\psi_4 = 15^\circ$
CA-HTLS	-0.411 ± 10.01	1.42 ± 72.18	0.350 ± 1.263	0.032 ± 22.91
MV-HTLS	-2.140 ± 12.82	-16.67 ± 64.87	-0.214 ± 1.146	1.022 ± 29.87
P0-HTLS	0.128 ± 13.46	11.76 ± 76.95	0.610 ± 1.495	1.310 ± 28.03
Method	$f_5 = 478\text{Hz}$	$d_5 = 808\text{Hz}$	$a_5 = 17.0\text{a.u.}$	$\psi_5 = 15^\circ$
CA-HTLS	1.82 ± 20.68	-7.90 ± 129.3	-0.069 ± 2.336	-0.171 ± 6.581
MV-HTLS	-13.19 ± 20.19	-18.31 ± 112.5	-0.298 ± 2.061	2.840 ± 6.003
P0-HTLS	6.49 ± 24.58	-28.87 ± 128.8	-0.439 ± 2.470	-0.394 ± 7.332

interfering peaks. As shown in Fig.2, the resolution is doubled compared to Cadzow's method that still performs better than the nonenhanced method P0-HTLS. All detected failures in resolution are due to the fact that an interfering peak, mostly peak 4, can not be resolved.

As shown in Table 1, differences in *accuracy of the estimated parameters* between the methods under study are small, especially for peak 1, 2 and 3. The damping factors and amplitudes of peak 4 and 5 and also the phase of peak 5 are better estimated by MV-HTLS but the frequencies are estimated more accurately by CA-HTLS. This loss in accuracy is due to the occurrence of a smaller singular value gap σ_K/σ_{K+1} in the 119×10 data matrix H used by MV-HTLS compared to the one in the 65×64 matrix used in CA-HTLS, thereby also increasing the bias of the estimates. On the other hand, increasing the number of columns M of H from 6 to 64 (square), first decreases and then increases –from $M = 15$ on– the failure rate of MV-HTLS from 10% to 20% while the accuracy of all estimates remains more or less the same for all M values. Therefore, we better take M small ($\approx 2K$) since a higher M does not improve the performance.

Furthermore, no differences in accuracy or resolution have been ob-

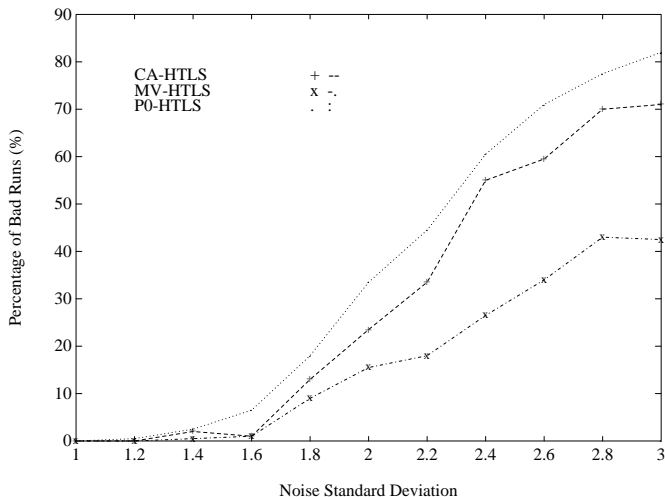


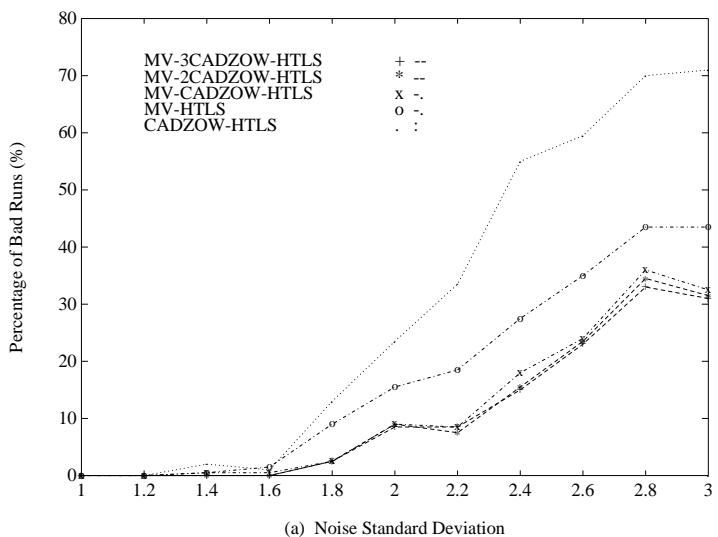
Figure 2. Percentage of times that P0-HTLS, CA-HTLS and MV-HTLS fail to resolve all peaks of Example 1 versus the noise standard deviation σ_v .

served between the use of the exact *noise variance* in the correction function of MV-HTLS and the use of one of the estimators (as given in Sec.2).

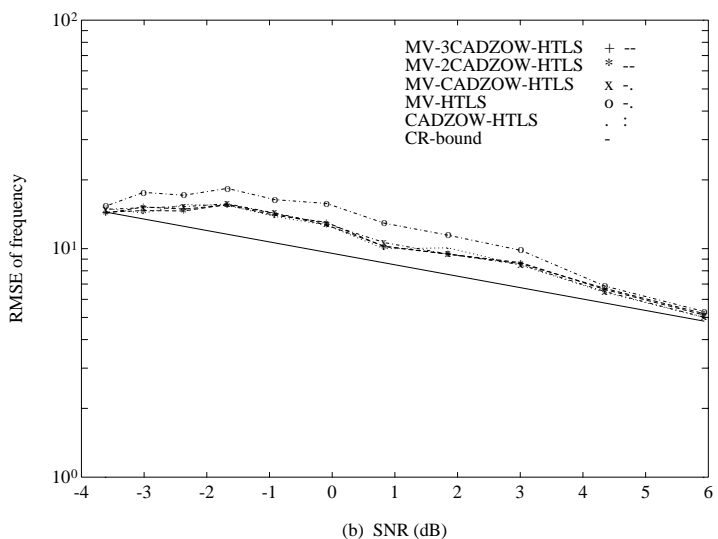
Overestimating the model order (choosing the order > 5) further improves clearly the failure rate (not the accuracy) of all methods, but the differences in failure rate remain relatively the same.

Finally, we can apply the signal enhancement algorithm *iteratively* or combine several algorithms. As shown in Fig.3, applying the MV estimation method followed by a Cadzow iteration prior to HTLS, called MV-CADZOW-HTLS, reduces further the failure rate and also improves the parameter accuracy wherever CA-HTLS performs better.

Similar experiments have been performed using the signal parameter estimation algorithm HSVD but, except for the fact that the accuracy of the HTLS estimates is generally better than that of the HSVD estimates, the same conclusions hold. Another simulation example is described in (Van Huffel 1992). Similar observations as for Example 1 have been made except that here MV-HTLS exhibits a slightly better or comparable accuracy for all parameter estimates.



(a) Noise Standard Deviation



(b) SNR (dB)

Figure 3. Comparison of CA-HTLS, MV-HTLS and the iterated methods MV-CADZOW-HTLS, MV-2CADZOW-HTLS and MV-3CADZOW-HTLS (i.e. MV followed by 1,2 and 3 Cadzow iterations) for Example 1: (a) percentage of times that each method fails to resolve all peaks versus the noise standard deviation σ_ν (b) RMSE values, obtained for estimating $f_4 = 353$ Hz versus the peak SNR = $10 \log(a_4^2/(2\sigma_\nu^2))$. The solid line is the Cramér-Rao bound.

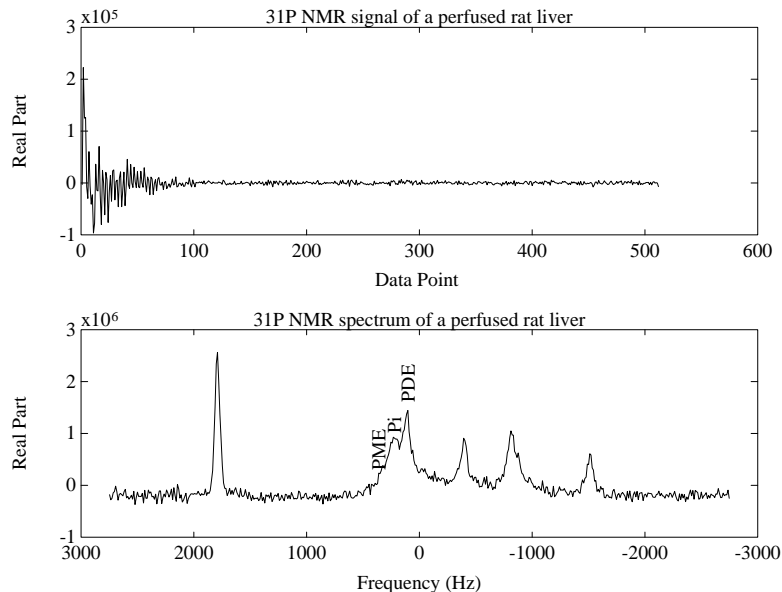


Figure 4. In vivo ^{31}P -NMR signal of Example 2 and its spectrum.

4 Application to NMR signal fitting

Finally, we apply MV-HTLS and P0-HTLS to the quantitative analysis of in vivo signals in NMR spectroscopy. The measurement data are assumed to be modeled by function (2.2) and perturbed by additive white noise. Furthermore, $t_n = t_0 + n\Delta t$ in which t_0 is the time lag between the effective origin and the first data point included in the analysis and Δt the sample interval. Because of this time delay, the signal parameters estimated by HTLS must be extrapolated to the time origin.

Example 2. Fig.4 shows the ^{31}P -NMR signal from a perfused rat liver, which was obtained in a 4.7 Tesla, 30 cm-wide bore magnet, equipped with a Biospec spectrometer, and acquired at 81.1 MHz. 128 scans were accumulated using $60 \mu\text{s}$ (72°) pulses with a 0.69s repetition time. The peaks of interest are PDE (phospho-diester), Pi (anorganic phosphate) and PME (phospho-monoester). The peak at high frequency is a standard compound with known concentration and frequency so that the concentration of the other peaks can be estimated absolutely instead of relatively from the computed amplitudes (extrapolated to the time origin). 150 data points are taken, starting from the 6th measurement on (the first 5 are deleted in order to eliminate the broad hump that appears in the original spectrum).

Table 2. The signal parameters corresponding to the 3 exponentially damped sinusoidal components that fit the peaks PDE-Pi-PME and extrapolated to the time origin, as estimated by P0-HTLS and MV-HTLS. $\psi_k = \phi_k * 180/\pi$ expresses the phase in degrees.

Peak	Method	f_k (Hz)	d_k (Hz)	a_k (a.u.)	ψ_k (deg.)
PDE	P0-HTLS	102.08	196.91	37715.64	3.43
	MV-HTLS	95.35	266.13	69178.07	10.07
Pi	P0-HTLS	236.35	257.16	24323.91	-44.44
	MV-HTLS	225.41	397.28	60455.14	-3.86
PME	P0-HTLS	322.14	672.51	69439.97	-44.34
	MV-HTLS	318.20	324.92	13521.72	12.93

The data are arranged in a 129×22 Hankel matrix during preprocessing when using MV-HTLS. The model order is set to 15.

The better fit of MV-HTLS compared to P0-HTLS of the 3 interfering peaks PDE-Pi-PME is visualized in Fig.5 by drawing the exponentially damped sinusoidal components that fit each peak separately. Table 2 yields the computed estimates, extrapolated to time zero. The smaller damping factor of PME and phases close to zero, corresponding to physical reality, clearly indicate that MV-HTLS produces the best fit and hence the most accurate estimates.

5 Conclusions

A new signal enhancement algorithm based on minimum variance estimation is given demonstrating a significant improvement in resolution performance and computational efficiency over Cadzow's method at a comparable parameter accuracy.

Acknowledgement: the author is a Research Associate of the Belgian N.F.W.O. (National Fund for Scientific Research).

Bibliography

1. Cadzow, J. (1988). Signal enhancement: a composite property mapping algorithm. *IEEE Trans. on Acoust., Speech, and Sign. Proc.*, *ASSP-36*, 49–62.
2. Cadzow, J. A. and Wilkes, D. M. (1991). Enhanced sinusoidal and exponential data modeling. In *SVD and Signal Processing, II: Algorithms, Analysis and Applications* (ed.: Vaccaro, R. J.). Elsevier Science Publishers B.V., Amsterdam, 335–352.

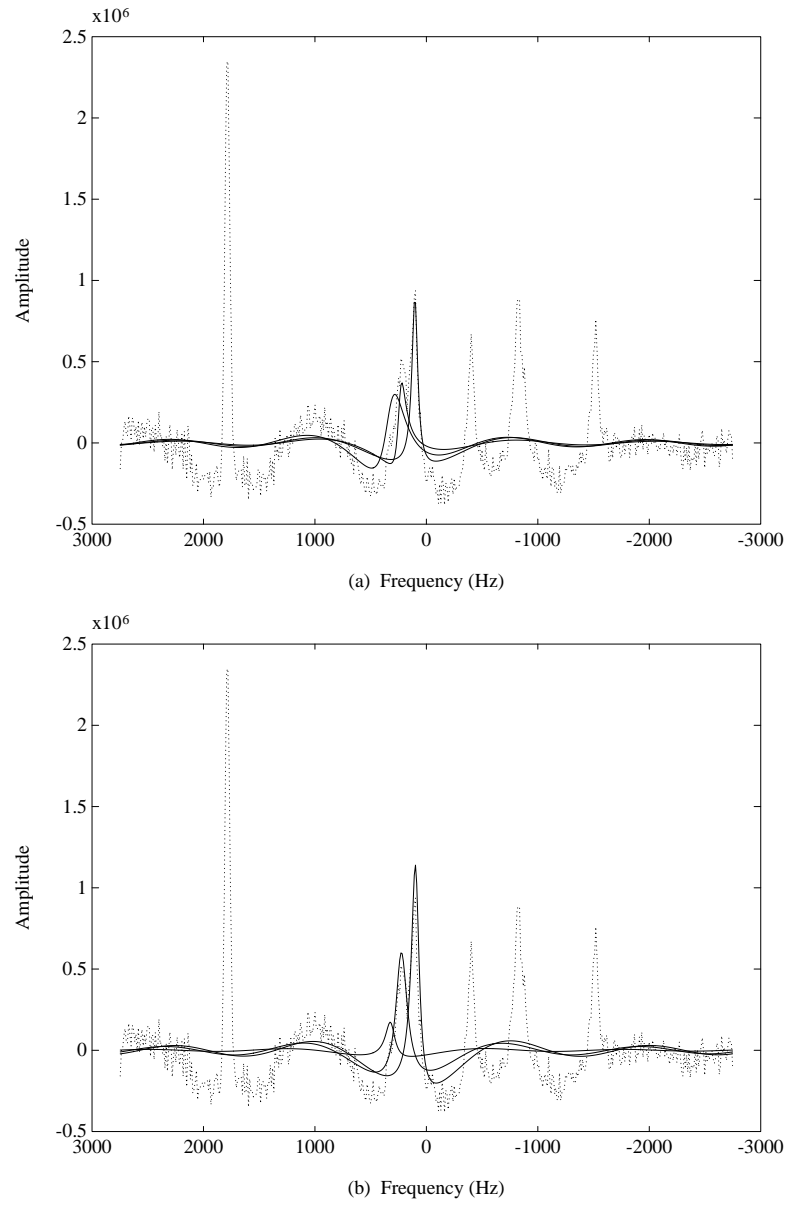


Figure 5. The spectra of the exponentially damped sinusoidal components that reconstruct the 3 interfering peaks PDE-Pi-PME of the signal in Fig.4, as computed by (a) P0-HTLS (b) MV-HTLS.

3. De Beer, R. and Van Ormondt, D. (1991). Analysis of NMR data using time-domain fitting procedures. In *In-vivo Magnetic Resonance Spectroscopy I: Probeheads, Radiofrequency Pulses, Spectrum Analysis* (guest ed.: Rudin, M.). NMR Basic Principles and Progress series, Vol.26, Springer-Verlag, Berlin Heidelberg, 201–248.
4. De Moor, B. (1993). The singular value decomposition and long and short spaces of noisy matrices. *IEEE Trans. on Sign. Proc.*, to appear.
5. Golub, G. H. and Van Loan, C. F. (1989). *Matrix computations* (2nd edn), The Johns Hopkins University Press, Baltimore, Maryland.
6. Kumaresan, R. and Tufts, D. W. (1982). Estimating the parameters of exponentially damped sinusoids and pole-zero modeling in noise. *IEEE Trans. on Acoust., Speech, and Sign. Proc.*, *ASSP-30*, 833–840.
7. Kung, S. Y., Arun, K. S. and Rao, D. V. B. (1983). State-space and singular value decomposition-based approximation methods for the harmonic retrieval problem. *J. Opt. Soc. Am.*, *73*, 1799–1811.
8. Tufts, D., Kumaresan, R. and Kirsteins, I. (1982). Data adaptive signal estimation by singular value decomposition of a data matrix. *Proc. IEEE*, *70*, 684–685.
9. Van Huffel, S. (1993). Enhanced resolution based on minimum variance estimation and exponential data modeling. *Signal Processing*, to appear.
10. Van Huffel, S. and Vandewalle, J. (1991). *The total least squares problem : computational aspects and analysis*. Frontiers in Applied Mathematics series, Vol.9, SIAM, Philadelphia.
11. Van Huffel, S., Aerts, L., Bervoets, J., Vandewalle, J., Decanniere, C. and Van Hecke, P. (1992). Improved quantitative time-domain analysis of NMR data by total least squares. In *Signal Processing VI: theories and applications. Proceedings 6th European Sign. Proc. Conf. (EU-SIPCO)* (eds.: Vandewalle, J., Boite, R., Moonen, M. and Oosterlinck, A.). Elsevier Science Publishers B.V. (North-Holland), Vol. III, 1721–1724.